Analyzing the Impact of Evolving Combustion Conditions on the Composition of Wildfire Emissions Using Satellite Data

Anderson, Lindsey D.; Dix, Barbara; Schnell, Jordan; Yokelson, Robert; Veefkind, J. Pepijn; Ahmadov, Ravan; de Gouw, Joost

DOI
10.1029/2023GL105811

Publication date
2023

Document Version
Final published version

Published in
Geophysical Research Letters

Citation (APA)
Anderson, L. D., Dix, B., Schnell, J., Yokelson, R., Veefkind, J. P., Ahmadov, R., & de Gouw, J. (2023). Analyzing the Impact of Evolving Combustion Conditions on the Composition of Wildfire Emissions Using Satellite Data. *Geophysical Research Letters*, *50*(23), Article e2023GL105811. https://doi.org/10.1029/2023GL105811

Geophysical Research Letters

RESEARCH LETTER
10.1029/2023GL105811

Analyzing the Impact of Evolving Combustion Conditions on the Composition of Wildfire Emissions Using Satellite Data

Lindsey D. Anderson[1,2], Barbara Dix[2], Jordan Schnell[2,3], Robert Yokelson[4], J. Pepijn Veefkind[5,6], Ravan Ahmadov[3], and Joost de Gouw[1,2]

[1]Department of Chemistry, University of Colorado Boulder, Boulder, CO, USA, [2]Cooperative Institute for Research in Environmental Sciences (CIRES), University of Colorado Boulder, Boulder, CO, USA, [3]NOAA Global Systems Laboratory, Boulder, CO, USA, [4]Department of Chemistry, University of Montana, Missoula, MT, USA, [5]Royal Netherlands Meteorological Institute, de Bilt, The Netherlands, [6]Department of Geoscience and Remote Sensing, Delft University of Technology, Delft, The Netherlands

Key Points:

- Space-based remote sensing instruments can be used to observe changes in the composition of wildfire emissions over time
- Changes in wildfire emissions composition observed with TROPOMI were caused by evolving combustion conditions rather than aerosol shielding
- TROPOMI observations can be used to help parametrize how modeled wildfire emissions should change with evolving combustion conditions

Supporting Information:

Supporting Information may be found in the online version of this article.

Correspondence to:

J. de Gouw,
joost.degouw@colorado.edu

Citation:

Anderson, L. D., Dix, B., Schnell, J., Yokelson, R., Veefkind, J. P., Ahmadov, R., & de Gouw, J. (2023). Analyzing the impact of evolving combustion conditions on the composition of wildfire emissions using satellite data. *Geophysical Research Letters*, *50*, e2023GL105811. https://doi.org/10.1029/2023GL105811

Received 9 AUG 2023
Accepted 18 NOV 2023

Abstract Wildfires have become larger and more frequent because of climate change, increasing their impact on air pollution. Air quality forecasts and climate models do not currently account for changes in the composition of wildfire emissions during the commonly observed progression from more flaming to smoldering combustion. Laboratory measurements have consistently shown decreased nitrogen dioxide (NO_2) relative to carbon monoxide (CO) over time, as they transitioned from more flaming to smoldering combustion, while formaldehyde (HCHO) relative to CO remained constant. Here, we show how daily ratios between column densities of NO_2 versus those of CO and HCHO versus CO from the Tropospheric Monitoring Instrument (TROPOMI) changed for large wildfires in the Western United States. TROPOMI-derived emission ratios were lower than those from the laboratory. We discuss reasons for the discrepancies, including how representative laboratory burns are of wildfires, the effect of aerosols on trace gas retrievals, and atmospheric chemistry in smoke plumes.

Plain Language Summary Climate change has led to an increase in the frequency and size of wildfires in the Western United States. The gases and particles released from wildfires impact air quality and climate, so it is important to understand the chemical composition of these emissions. In current air quality forecasts and climate models, the composition of wildfire emissions is based on the dominant vegetation burned and is assumed to be constant over time. In contrast, measurements from laboratory burns indicate that the composition of emissions from fires changes over time, as fires progress from more flaming combustion to flameless burning dominated by smoke (smoldering). It is challenging to have daily field measurements of the emissions from long-lived wildfires, but there are instruments in space that can make daily observations of wildfires globally. In this study, we show how the composition of emissions from wildfires in California, Oregon, and Washington changed over time, as they progressed from more flaming to more smoldering combustion, using observations from a satellite instrument called TROPOMI. The analysis of the composition of wildfire emissions and their evolution over time using TROPOMI could improve air quality forecasting and climate modeling globally.

1. Introduction

The buildup of fuel from fire suppression practices and anthropogenic climate change has doubled the area burned annually in the Western United States since the mid-1980s, compared to that expected from natural climate variability (Abatzoglou & Williams, 2016; Balch et al., 2017; Dennison et al., 2014; Westerling et al., 2006). Wildfire emissions negatively impact human health (Grant & Runkle, 2022; Reid et al., 2016), affect the formation of ozone downwind (Jaffe & Wigder, 2012; Xu et al., 2021), and influence the climate (Abatzoglou & Williams, 2016), highlighting the need for a comprehensive understanding of wildfire emissions to inform air quality forecasts and climate models (Sokolik et al., 2019). Most air quality forecasts and climate models assume that the chemical composition of wildfire emissions depends only on the vegetation type and area burned (van der Werf et al., 2017). However, laboratory and field measurements indicate that the composition of wildfire emissions are also dependent on the dominant combustion type (flaming vs. smoldering, Akagi et al., 2011; Burling et al., 2011; Liu et al., 2017; Roberts et al., 2020; Sekimoto et al., 2018; Selimovic et al., 2018; Yates

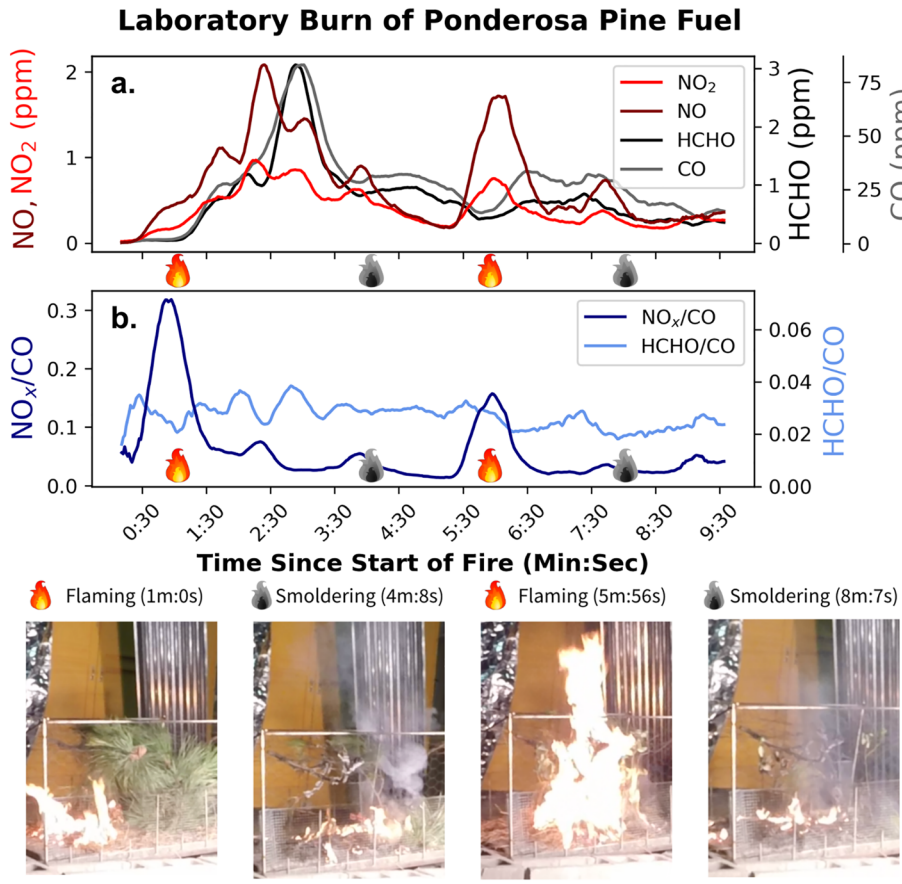

Figure 1. Data from Fire 37 of the FIREX FireLab study presented with a 15s moving average. Five minutes into the burn, dry ponderosa pine needles were added, so there were two distinct flaming and smoldering phases.

et al., 2016; Yokelson et al., 1996). A more complete understanding of the composition of wildfire emissions and their temporal evolution could improve air quality forecasts and climate models.

Results from the 2016 Fire Influence on Regional and Global Environments Experiment (FIREX) FireLab study illustrate the distinct composition of emissions during the flaming and smoldering phases of laboratory burns (Roberts et al., 2020; Sekimoto et al., 2018; Selimovic et al., 2018). As an example, Figure 1a shows that nitrogen monoxide (NO) and nitrogen dioxide (NO_2) emissions are dominant during periods characterized by more flaming combustion (1m:0s and 5m:56s), while carbon monoxide (CO) and formaldehyde (HCHO) are co-emitted by relatively inefficient smoldering combustion (4m:8s and 8m:7s). As a result, NO_x/CO (NO_x = NO + NO_2) decreases as the fire progresses from more flaming to more smoldering combustion (Figure 1b), while HCHO/CO does not change very much throughout the burn (Figure 1b). It is also important to note that flaming and smoldering combustion occur simultaneously throughout the transition from predominantly flaming to predominantly smoldering combustion (Figure 1a).

While field-based measurements provide the most detailed information about the chemical composition of wildfire smoke, their availability is limited. This makes it challenging to characterize the emissions from an individual wildfire over days to weeks, as it evolves from more flaming to more smoldering combustion. Satellite remote sensing has the potential to characterize temporal changes in emissions for many more wildfires globally. While only a few trace gases can be detected from space, this subset includes compounds that are predominantly from flaming combustion (NO_2, nitrous acid (HONO)) versus some that are predominantly released from smoldering (CO, HCHO, glyoxal (CHOCHO), ammonia (NH_3)). Several studies have used satellite data to quantify the emission of air pollutants from wildfires. Emissions estimates using high resolution (~3.5 × 5.5 km^2) NO_2 measurements from the Tropospheric Monitoring Instrument (TROPOMI) were found to be consistent with those calculated using field-based measurements (Griffin et al., 2021; Jin et al., 2021). The ratio between NO_2 and CO

from TROPOMI has been used as a proxy for wildfire combustion efficiency (van der Velde et al., 2021). Additionally, TROPOMI has been used to detect HONO enhancement in fresh wildfire smoke (Theys et al., 2020), and the ratio between TROPOMI HONO and NO_2 has been found to increase with increasing fire radiative power (Fredrickson et al., 2023).

In this study, we used TROPOMI to investigate changes in trace gas ratios ($\Delta NO_2/\Delta CO$ and $\Delta HCHO/\Delta CO$) from wildfires over the course of multiple weeks, finding they progressed from more flaming to more smoldering combustion. In dense smoke plumes, NO_2 from TROPOMI can be underestimated by up to a factor of 6 (Rowe et al., 2022), an effect often referred to as aerosol shielding. This underestimation in NO_2 is due to light extinction from biomass burning aerosols in the ultraviolet and visible wavelength range, which is not fully accounted for in the operational NO_2 product from TROPOMI (van Geffen et al., 2022). Additionally, chemical transformation of air pollutants within a wildfire plume can be efficient (Calahorrano et al., 2021; Juncosa Calahorrano et al., 2021; Lindaas et al., 2021; Xu et al., 2021) and should be accounted for when determining trace gas ratios with satellite measurements. To address these challenges, we analyze the impact of aerosol shielding through radiative transfer analysis and the impact of chemistry on TROPOMI-derived trace gas ratios.

2. Data and Methodology

2.1. Fire Selection

The wildfires studied took place in California, Oregon, and Washington during the 2020 (6 fires) and 2021 (9 fires) wildfire seasons (Table S1, Figure S1a in Supporting Information S1). These wildfires were chosen because they were large (>100,000 acres) and burned for multiple weeks, allowing for the analysis of how their emissions changed over time. The starting locations and total burned area of the wildfires studied were gathered from InciWeb, a US Forest Service (USFS) database, and the California Department of Forestry and Fire Protection (CalFire).

2.2. TROPOMI and FRP Data

TROPOMI is a polar-orbiting spectrometer onboard the European Copernicus Sentinel-5 Precursor satellite that takes daily afternoon (~1:30 p.m. local time) measurements globally of spectral bands in the ultraviolet (UV), visible (Vis), near-infrared (NIR), and shortwave infrared (SWIR) regions of the electromagnetic spectrum (Veefkind et al., 2012). These wavelength bands allow for the observation of molecules and aerosols in wildfire plumes including NO_2 (van Geffen et al., 2022), HCHO (De Smedt et al., 2021), CO (Landgraf et al., 2016), and aerosol optical depth (AOD, Torres et al., 2020). TROPOMI has a spatial resolution up to ~3.5×5.5 km^2 in the UV-Vis and ~5.5×7 km^2 in the SWIR. Daily tropospheric column densities of NO_2 and HCHO, and total column densities of CO measured with TROPOMI were gridded to a ~7×7 km^2 (0.06×0.06 degree^2) resolution. We used versions 1 and 2 of offline level 2 NO_2 and CO data, and we used version 2 of offline level 2 HCHO data. TROPOMI AOD at 388 nm was averaged with an area weight over a 0.06×0.06 degree^2 spatial grid to match the trace gas data. Using the Ångström component from the aerosol data file, the gridded AOD was interpolated to 437.5 nm to be near the center wavelength of the NO_2 analysis window used by TROPOMI (van Geffen et al., 2022).

The quality assurance (qa) thresholds used for NO_2, HCHO, and CO respectively were 0.50, meaning that only TROPOMI pixels with a higher qa value were included in the analysis (data filtering is further explained in Text S1 of the Supporting Information S1). AOD data was included when the quality flag was a 0 or 1. Fire radiative power (FRP) measurements from the National Aeronautics and Space Administration (NASA) and the National Oceanic and Atmospheric Administration (NOAA) Visible Infrared Imaging Radiometer Suite (VIIRS) instrument onboard the Suomi National Polar-Orbiting Partnership (S-NPP, closely co-located with TROPOMI) spacecraft were filtered to include daytime measurements (~1:30p.m. local time) with a nominal or high confidence designation.

The column densities of NO_2 and HCHO were compared against those of CO to account for dilution effects because CO is relatively inert and released during both flaming and smoldering combustion. Wildfires smaller than 1,000,000 acres were analyzed using satellite data in a ~100 km × 100 km (~1×1 degree^2) bounding box centered at the initial wildfire location, while larger wildfires were analyzed with a ~200 km × 200 km (~2×2 degree^2) bounding box (Table S1 in Supporting Information S1).

2.3. Fuel Type Analysis

The fuel types burned in each wildfire were identified using the satellite-based land cover and fuel classification in version 4 of the Global Fire Emission Database (GFED4s), which is described in van der Werf et al. (2017). The GFED4s has monthly dry matter (DM) emissions and includes the contribution from different fuel types at a 0.25×0.25 degree^2 spatial resolution. Data from the starting month of each wildfire was filtered using the same bounding boxes as those for the trace gas analysis (Table S1 in Supporting Information S1). The fraction of each fuel type responsible for total DM emissions during this month was calculated. The fuel types present included agriculture, savanna (including grassland or shrubland), and temperate forest designations (Figure S1b in Supporting Information S1).

2.4. Radiative Transfer Modeling Analysis and RAP-Chem Data

To assess the sensitivity of satellite-derived $\Delta NO_2/\Delta CO$ ratios to aerosols present in the smoke plumes, we calculated the satellite's measurement sensitivity for different aerosol scenarios throughout the Beckwourth Complex Fire (Section 3.3). Simulated daily profiles of NO_2, CO, and aerosol extinction from the Rapid-Refresh model coupled to Chemistry (RAP-Chem) were used as input to the Monte Carlo Atmospheric Radiative Transfer Model (McArtim) version 3 (Deutschmann et al., 2011). The RAP-Chem is an experimental air quality forecast model that combines dynamics and physics from the Rapid-Refresh forecast model (Benjamin et al., 2016) with the Weather Research and Forecasting model coupled with Chemistry (WRF-Chem, Grell et al., 2005). Emission factors used in RAP-Chem are based on those in Andreae (2019). Full details are provided in Texts S2 and S3 and Table S2 of the Supporting Information S1.

3. Results and Discussion

Below we show that TROPOMI can be used to monitor changes in the composition of wildfire emissions as combustion conditions evolve. First, we analyze how $\Delta NO_2/\Delta CO$ and $\Delta HCHO/\Delta CO$ ratios from TROPOMI changed throughout the Beckwourth Complex Fire as a case study. Then, we extend the analysis for 15 large wildfires. Finally, we discuss how aerosol shielding and chemistry impacted TROPOMI-derived trace gas emission ratios.

3.1. Changes in the Composition of Emissions During the Beckwourth Complex Fire

The Beckwourth Complex Fire, which burned over 100,000 acres in northern California, is used here to illustrate temporal changes in wildfire emissions observed by TROPOMI. On the first day the wildfire was detected from space (Day 0), the NO_2 tropospheric column density and CO total column density were elevated over the active fire region (Figures 2a and 2b), indicated by FRP measurements, which can be used as a proxy for combustion intensity. More than a week after the start of the wildfire (Day 8), the NO_2 had decreased over the active fire region (Figure 2c), while the CO remained moderately elevated (Figure 2d). The $\Delta NO_2/\Delta CO$ ratio was derived from a linear regression analysis of tropospheric NO_2 against total column CO, where the slope is the enhancement ratio. To determine whether TROPOMI can observe differences in the composition of emissions at different stages of the wildfire, $\Delta NO_2/\Delta CO$ calculated on Day 0 and Day 8 of the Beckwourth Complex Fire were compared (Figure 2e). The $\Delta NO_2/\Delta CO$ was twice as large on Day 0 as it was on Day 8, which is consistent with FRP measurements decreasing with time, as the wildfire transitioned from more flaming to more smoldering combustion (Figure 2f).

Following the example shown in Figure 2, $\Delta NO_2/\Delta CO$ was determined for each day of the Beckwourth Complex Fire. There was a decrease in $\Delta NO_2/\Delta CO$ throughout the wildfire, and the data was fit with an exponential decay because the $\Delta NO_2/\Delta CO$ cannot physically be less than 0 (Figure S3a in Supporting Information S1). Daily variations in $\Delta NO_2/\Delta CO$ were likely caused by changes in fire behavior, such as spreading of the wildfire to unburned areas or changes in fuel type (Burling et al., 2010; Roberts et al., 2020), which also affects FRP (Wooster et al., 2011, Figures S3b and S3c in Supporting Information S1). In Figure S3b of the Supporting Information S1 we show average FRP, which is the average of the FRP measurements inside the same bounding box used in the TROPOMI analysis, throughout the Beckwourth Complex Fire. The overall decrease in both $\Delta NO_2/\Delta CO$ and average FRP over time (Figures S3a and S3b in Supporting Information S1) indicates that TROPOMI can be used

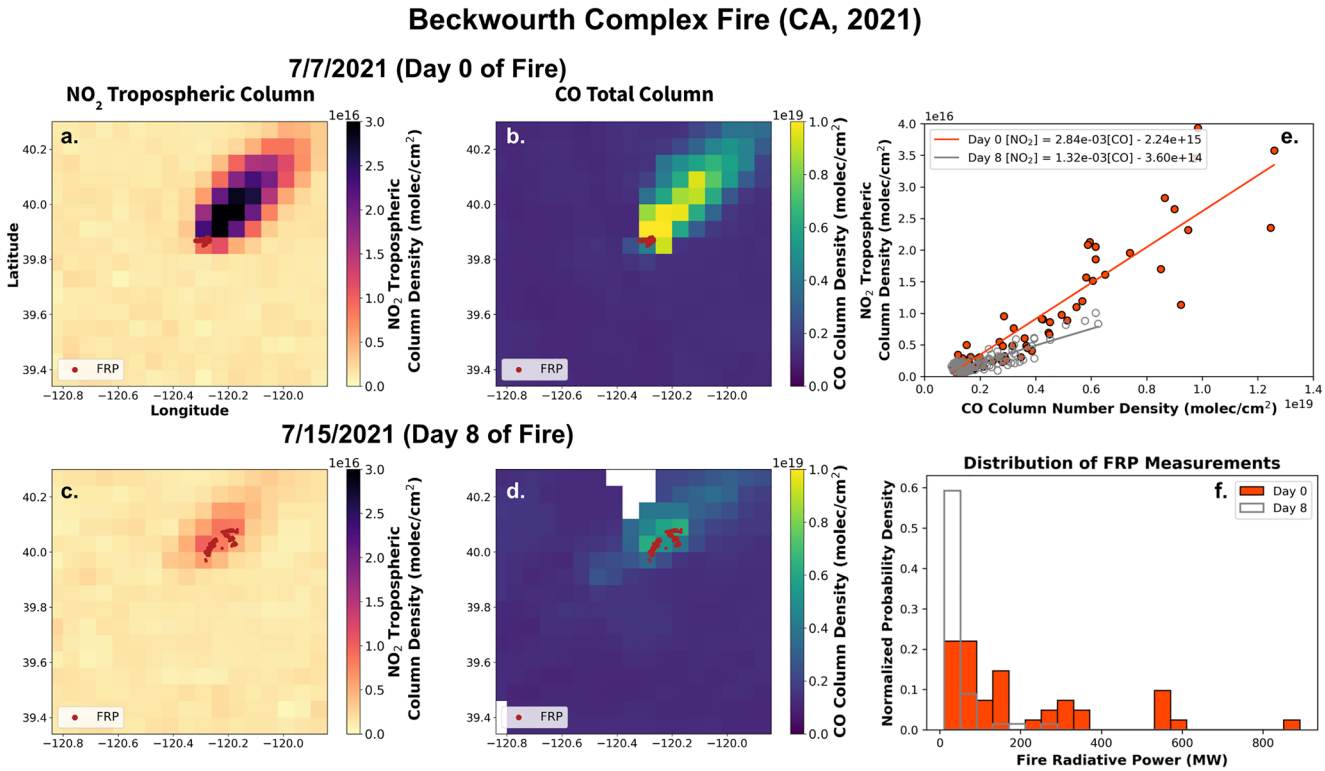

Figure 2. (a, c) NO_2 and (b, d) CO from TROPOMI on Day 0 and Day 8 of the Beckwourth Complex Fire. Red pixels on (a)–(d) show FRP measurements from VIIRS. (e) NO_2 values for each pixel plotted against CO values 0 (orange) and 8 days (gray) after the start of the wildfire. (f) Distribution of FRP measurements on Day 0 (orange) and Day 8 (gray) of the wildfire. VIIRS S-NPP true color images of the wildfire plumes on Day 0 and Day 8 can be seen in Figure S2 of the Supporting Information S1.

to analyze how the composition of wildfire emissions evolved as the Beckwourth Complex Fire transitioned from more flaming to more smoldering combustion.

3.2. Changes in the Composition of Emissions for All Fires

Trace gas emission ratio analysis was repeated for 15 large (>100,000 acres) wildfires in California, Oregon, and Washington during the 2020 and 2021 wildfire seasons (Figure S1a, Table S1 in Supporting Information S1). Daily $\Delta NO_2/\Delta CO$ and average FRP measurements decreased throughout the course of these wildfires as they progressed from more flaming combustion to more smoldering combustion (Figures 3a and 3b). Overall, the decrease in $\Delta NO_2/\Delta CO$ over time was consistent across all fuel types analyzed (Figure S4 in Supporting Information S1). There were days when the $\Delta NO_2/\Delta CO$ increased compared with the day before; these increases often correlated with increased average FRP (Figure 3c; Figure S5a in Supporting Information S1). Figure 3c indicates that average FRP can be used to help estimate how $\Delta NO_2/\Delta CO$ changed throughout the course of several wildfires. However, we also find that the age of the fire is an important parameter in understanding the evolution of wildfire emissions.

The numerical values of $\Delta NO_2/\Delta CO$ from TROPOMI (Figure 3a) are smaller than $\Delta NO_x/\Delta CO$ from the laboratory and field by a factor of 2–20 (Table S3 in Supporting Information S1), partially due to aerosol shielding. We compare $\Delta NO_2/\Delta CO$ from space with $\Delta NO_x/\Delta CO$ from the laboratory and field because most of the emitted NO_x would become NO_2 on the spatial scales relevant to the satellite measurements. The $\Delta NO_x/\Delta CO$ from the laboratory and field decreases with decreasing modified combustion efficiency (MCE, Table S3 in Supporting Information S1), which is consistent with the downward trend in TROPOMI $\Delta NO_2/\Delta CO$ over time (Figure 3a). The MCE is calculated based on the enhancement of carbon dioxide compared with the sum of the enhancement of carbon monoxide and the enhancement of carbon dioxide ($MCE = \Delta CO_2/(\Delta CO + \Delta CO_2)$, Yokelson et al., 1996). When the MCE is above 0.9, the emissions are from mainly flaming combustion, while MCE values less than 0.9

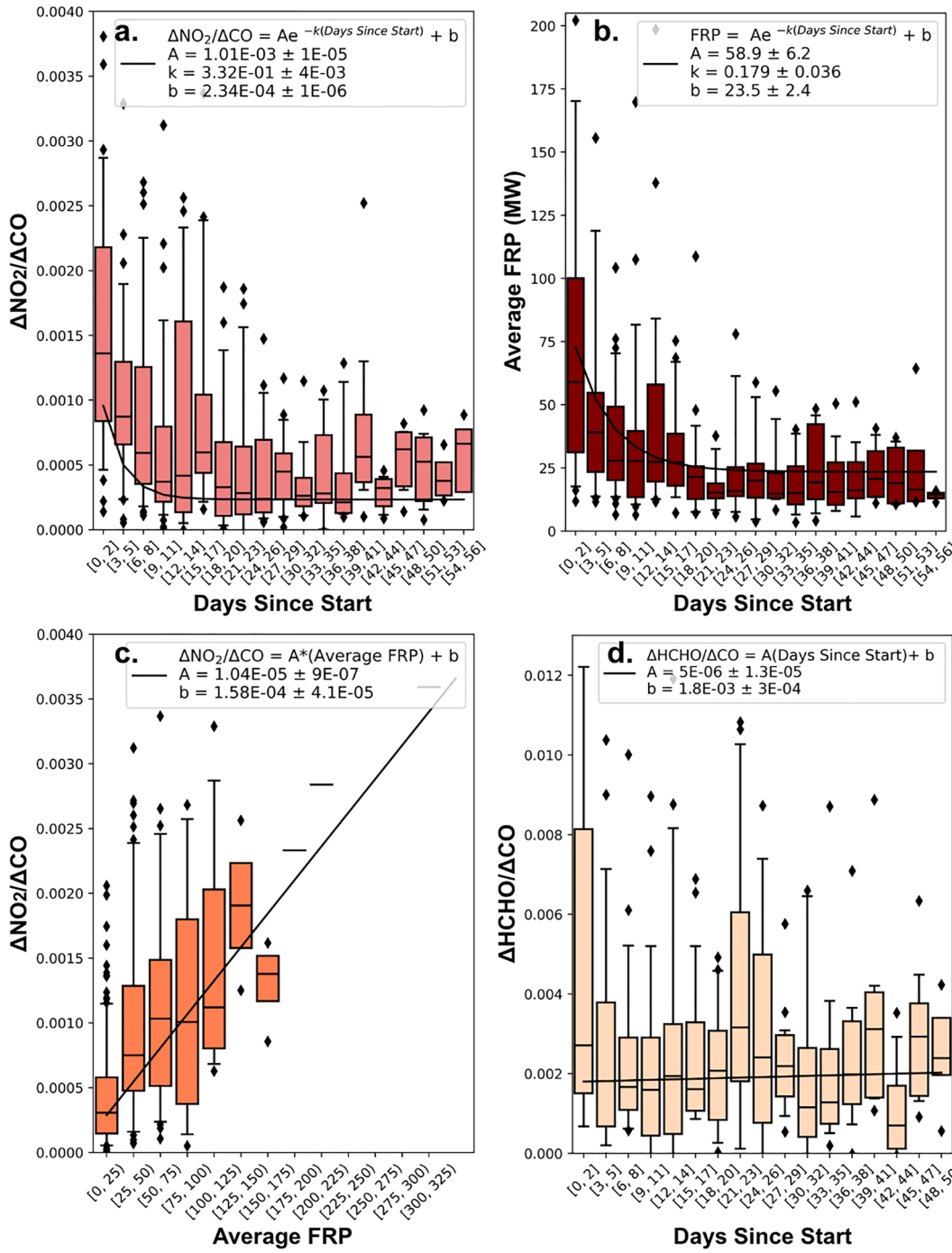

Figure 3. (a) $\Delta NO_2/\Delta CO$ over time, (b) FRP averaged over the same bounding box used in the TROPOMI analysis, (c) $\Delta NO_2/\Delta CO$ compared with average FRP, and (d) $\Delta HCHO/\Delta CO$ over time throughout the course of 15 large wildfires (Table S1 in Supporting Information S1). Error bars represent the 5th to 95th percentiles of each bin, and the regression lines on (a), (c), and (d) are inversely weighted by the standard deviation of the slopes included in the fit. The values with higher $\Delta NO_2/\Delta CO$ in (a) and (c) had more error, so the fitted lines were pulled down toward lower $\Delta NO_2/\Delta CO$ values.

indicate mainly smoldering combustion (Bertschi et al., 2003; Yokelson et al., 1996). However, MCE cannot be calculated using data from TROPOMI, so we use FRP as a proxy for changes in combustion intensity.

Wildfires analyzed that had HCHO data from TROPOMI (Table S1 in Supporting Information S1) were used to determine how HCHO changed relative to CO over time. In contrast with $\Delta NO_2/\Delta CO$, the $\Delta HCHO/\Delta CO$

ratios were relatively constant throughout the wildfires studied (Figure 3d) and did not correlate with average FRP (Figure S5b in Supporting Information S1). This is consistent with laboratory studies showing that HCHO and CO are co-emitted during mostly smoldering combustion. The ΔHCHO/ΔCO ratios from TROPOMI are smaller than those determined in the laboratory and in the field by a factor of 5–10 (Table S4 in Supporting Information S1). Some of this difference is due to an underestimation in HCHO. When HCHO column densities from TROPOMI are above 8×10^{15} molec. cm^{-2}, which they are in the wildfire plumes analyzed, HCHO values are systematically 25% lower than ground-based column measurements (De Smedt et al., 2021). Additionally, HCHO from TROPOMI is analyzed using UV-Vis wavelengths, so HCHO retrievals are also impacted by aerosol shielding. However, ΔHCHO/ΔCO does not depend on MCE (Table S4 in Supporting Information S1), which is in agreement with the relatively consistent ΔHCHO/ΔCO over time from TROPOMI (Figure 3d).

Overall, we found a decrease in TROPOMI-derived $\Delta NO_2/\Delta CO$ throughout the course of several large wildfires, while ΔHCHO/ΔCO remained relatively constant, which agrees with expectations from FIREX FireLab studies. When comparing $\Delta NO_2/\Delta CO$ from TROPOMI with $\Delta NO_x/\Delta CO$ from the laboratory and the field (Table S3 in Supporting Information S1), numerical values are significantly smaller. Reasons for this discrepancy include:

1. Many sticks and leaves were burned during the FIREX FireLab study, which have a much higher (10–50×) nitrogen content than the wood commonly burned in Western U.S. wildfires (Coggon et al., 2016; Roberts et al., 2020). This decision was made, in part, because of the time it would have taken to burn larger fuel sources (e.g., 33 hr for a single log, Bertschi et al., 2003). We estimate that the choice of fuels could have inflated measurements of reactive nitrogen by more than 40%, compared to a more realistic ecosystem.
2. TROPOMI does not measure NO, so it misses out on a portion of NO_x measurements. While much of the NO is converted to NO_2 downwind of the fire, fresh emissions could have NO concentrations that are ∼20% of the NO_2 (Lindaas et al., 2021), and NO can still be present in aged wildfire plumes (Juncosa Calahorrano et al., 2021).
3. Underestimation of NO_2 from TROPOMI because of the impact of aerosol shielding on retrievals.
4. Chemical conversion of NO_x to different nitrogen-containing molecules in aging wildfire plumes (Calahorrano et al., 2021; Juncosa Calahorrano et al., 2021).

In the remainder of this paper, we discuss 3 and 4 more quantitatively, with a specific focus on whether these effects impacted the downward trend in $\Delta NO_2/\Delta CO$ that we observed over time.

3.3. Effect of Aerosols on $\Delta NO_2/\Delta CO$ From TROPOMI

In most cases, the presence of aerosols is negligible for the CO retrieval from TROPOMI (5%–10% overestimation), but can strongly affect the retrieved NO_2 vertical columns (Rowe et al., 2022). This is because with increasing AOD, the number of photons that pass through the entire wildfire plume and are reflected to the satellite sensor is reduced, leading to a potential underestimation in the NO_2 retrieval. To assess the impact of aerosols on $\Delta NO_2/\Delta CO$, we first compared AOD and NO_2 measurements on Day 0 and Day 8 of the Beckwourth Complex Fire. Even though the AOD was much higher on Day 0 compared with Day 8 (Figure S6 in Supporting Information S1), NO_2 was also significantly higher on Day 0 compared with Day 8 (Figures 2a and 2c). Plotting average NO_2 versus average AOD over all days of the fire shows that NO_2 is generally higher with higher AOD (Figure S7a in Supporting Information S1), despite the aerosol shielding effect. $\Delta NO_2/\Delta CO$ ratios show no negative correlation with AOD (Figure S7b in Supporting Information S1). Instead, higher $\Delta NO_2/\Delta CO$ correlates with higher FRP, which is indicative of its dependence on the stage of the fire. We conclude that while the aerosol shielding effect may reduce the observed NO_2 columns relative to the true values, the effect does not cause the trend of $\Delta NO_2/\Delta CO$ versus time and versus FRP (Figures 3a and 3c). If anything, the aerosol shielding effect may obscure some of the true dependence of $\Delta NO_2/\Delta CO$ ratios on time and FRP, meaning that for the Beckwourth Complex Fire, the decreasing trend in $\Delta NO_2/\Delta CO$ would be steeper without aerosol shielding.

Next, we quantitatively analyzed the impact of aerosol shielding on the magnitude of $\Delta NO_2/\Delta CO$ using RAP-Chem output for the Beckwourth Complex Fire and radiative transfer modeling (Texts S2–S4 and Figure S8 in Supporting Information S1). The RAP-Chem air quality forecast model uses constant emission ratios, so daily changes in modeled $\Delta NO_2/\Delta CO$ are caused by changes in plume chemistry or meteorology. The original $\Delta NO_2/\Delta CO$ calculated from RAP-Chem NO_2 and CO vertical column densities (VCDs) are shown together with the results of two aerosol case studies in Figure S8a of the Supporting Information S1. The first aerosol

case uses RAP-Chem AOD. However, the modeled AOD was significantly lower than the measured AOD, so in the second case, model AOD was scaled to get a magnitude comparable to the AOD observed by TROPOMI for the Beckwourth Complex Fire (Text S3 and Figures S7 and S8b in Supporting Information S1). For the aerosol case studies, satellite slant column densities (SCDs) and air mass factors (AMFs) for NO_2 were simulated with the radiative transfer model constrained by RAP-Chem. SCDs are the primary result of the spectroscopic analysis of TROPOMI data and are light-path dependent. Division of SCDs by AMF accounts for this and other dependencies, to yield universally comparable VCDs. Here, we converted NO_2 SCDs simulated for the wildfire plumes specific to each case study into VCDs using AMFs calculated for an aerosol free atmosphere (see Text S3 in Supporting Information S1). The $\Delta NO_2/\Delta CO$ calculated for these two aerosol case studies (Figure S8a in Supporting Information S1) present a worst-case scenario because the AMFs for the aerosol free atmosphere are larger than those accounting for aerosols within the plume. Resulting underestimation of the trace gas ratios for these two cases are on average a factor of 1.2 ± 0.1 using RAP-Chem AOD and 2.4 ± 0.5 for the scaled AOD case (Figure S8c in Supporting Information S1).

While aerosol shielding led to a decrease in magnitude of $\Delta NO_2/\Delta CO$, it had no significant effect on the trend over time, as indicated by line fits included in Figure S8a of the Supporting Information S1. We observed the overall trend in $\Delta NO_2/\Delta CO$ throughout the aerosol case studies instead of studying daily variability in $\Delta NO_2/\Delta CO$ because daily changes could be caused by differences in plume chemistry, meteorology, and aerosol shielding. For both the original data and the aerosol case studies, the trend over time remained flat, as expected, based on the constant emission ratios used in RAP-Chem. Overall, our analysis confirmed that the decrease in $\Delta NO_2/\Delta CO$ over time was not caused by the impact of aerosols on trace gas retrievals from TROPOMI.

3.4. Effect of Chemical Transformations in the Atmosphere

In order to determine the impact of chemistry on trace gas ratios from TROPOMI, we tested how the trace gas ratios changed as a function of bounding box size, that is, the domain used to calculate trace gas ratios, during the SQF Complex Fire (Table S1 in Supporting Information S1). As the bounding box size expanded and the number of pixels included in the analysis of the SQF Complex Fire increased, $\Delta NO_2/\Delta CO$ decreased due to the chemical removal of NO_2 (Figure S9a in Supporting Information S1, also observed in Jin et al. (2021) and Juncosa Calahorrano et al. (2021)). In contrast, $\Delta HCHO/\Delta CO$ increased with bounding box size because of HCHO formation downwind of the wildfire from the oxidation of organic molecules (Figure S9b in Supporting Information S1, also observed in Alvarado et al. (2020) and Liao et al. (2021)). In some cases, the bounding box size used for the SQF Complex Fire (1 degree^2) led to an observed underestimation of $\Delta NO_2/\Delta CO$ by up to a factor of 2, compared to $\Delta NO_2/\Delta CO$ observed at the smallest investigated bounding box size (0.16 degree^2). However, the smaller the bounding box size, the fewer pixels were available for the linear regression analysis used to determine trace gas ratios. For the SQF Complex fire, a bounding box of 1 degree^2 was chosen as a compromise between having enough data points available while minimizing the effect of chemistry on the trace gas ratios (Table S1 in Supporting Information S1). Overall, the observed underestimate in $\Delta NO_2/\Delta CO$ due to chemistry was 25%, while the observed overestimate in $\Delta HCHO/\Delta CO$ was 30%, when comparing the observed trace gas ratios at 1 degree^2 with those at 0.16 degree^2 (Figure S9 in Supporting Information S1).

4. Conclusions

Wildfires are projected to continue becoming larger and more frequent due to climate change, so it is important to have a comprehensive understanding of wildfire emissions and their temporal evolution to inform air quality forecasts and climate models. We have shown that the composition of wildfire emissions changed throughout the course of several wildfires in California, Oregon, and Washington. Emitted NO_2, which is predominantly from flaming combustion, decreased strongly over the course of several wildfires relative to CO. In contrast, HCHO relative to CO remained relatively constant because both are co-emitted during smoldering combustion. While these trends agree with those from FIREX FireLab experiments, the values from TROPOMI are lower due to differences in fuels burned, aerosol shielding, and chemistry.

Our work suggests that we can see changes in the emissions composition of large wildfires over time using daily trace gas measurements from TROPOMI. For these large wildfires, we also noted a correlation between the $\Delta NO_2/\Delta CO$ and the average FRP. Current air quality forecast models such as the RAP-Chem model and the

Rapid-Refresh Forecast System with Smoke and Dust (RRFS-SD) model use vegetation type and satellite FRP measurements to parameterize wildfire emissions. However, they do not currently have parameterizations for how emissions estimates should change based on the amount of flaming and smoldering combustion. Finding a parameterization that estimates the effect of the temporal evolution of wildfire emissions composition based on remote sensing measurements (e.g., trace gas ratios and average FRP) and weather could better inform models such as RRFS-Smoke and RAP-Chem.

Overall, we have shown that TROPOMI observed a significant decrease (around a factor of 4) in $\Delta NO_2/\Delta CO$ and relatively consistent $\Delta HCHO/\Delta CO$ throughout the course of several large wildfires, which agrees with overall trends observed in laboratory and field studies. These results are robust despite the impacts of aerosol shielding and chemistry on $\Delta NO_2/\Delta CO$ and $\Delta HCHO/\Delta CO$. We expect aerosol shielding to have a similar impact on $\Delta HCHO/\Delta CO$ as $\Delta NO_2/\Delta CO$. We estimate that aerosol shielding and chemistry could cause an underestimation of trace gas ratios by a factor of 2–3.

Even though there are many trace gases that cannot be observed from space, the ones that can be range from those dominant during flaming combustion (NO_2, HONO) to those dominant during smoldering (CO, HCHO, CHOCHO, NH_3). This allows us to gain valuable insight on how the composition of wildfire emissions change over time using space-based remote sensing instruments. TROPOMI measurements were used in Fredrickson et al. (2023) to study the ratio between HONO and NO_2 for intense wildfires with high average FRP. In contrast, we observed wildfires with lower average FRP to study the transition from mainly flaming to mainly smoldering combustion by comparing the ratio between NO_2 and CO. Looking forward, space-based remote sensing measurements of other trace gases from wildfires including HONO, CHOCHO, and NH_3 could be analyzed with respect to CO over time. Additionally, the Tropospheric Emissions: Monitoring of Pollution (TEMPO) instrument that launched in April of 2023 measures NO_2, HCHO, and other air pollutants at an unprecedented spatial ($\sim 2.1 \times 4.1$ km^2) and temporal (hourly during the day) resolution (Zoogman et al., 2017). Data from TEMPO will allow us to further understand the temporal evolution of wildfire emissions.

Data Availability Statement

Information on the wildfires analyzed in this study can be found online at InciWeb (https://inciweb.nwcg.gov/) and CalFire (https://www.fire.ca.gov/). InciWeb deletes information on the wildfires once they are considered no longer relevant, so a spreadsheet with information regarding the names, starting locations, and sizes of the wildfires analyzed in this study is available in Anderson et al. (2023). FRP statistics and TROPOMI enhancement ratios of $\Delta NO_2/\Delta CO$ and $\Delta HCHO/\Delta CO$ from the wildfires analyzed in this study are also available in Anderson et al. (2023). Rap-Chem model output data for the Beckwourth Complex Fire is available in Schnell and Ahmadov (2023).

Offline level 2 TROPOMI NO_2 (Copernicus Sentinel-5P, 2018b, 2021b), HCHO (Copernicus Sentinel-5P, 2020), and CO (Copernicus Sentinel-5P, 2018a, 2021a) data can be downloaded from the Copernicus Data Space Ecosystem (https://dataspace.copernicus.eu/). TROPOMI AOD at 388 nm is available in Torres (2021). To download the TROPOMI data used in this study, we recommend using the wildfire starting locations and date ranges described in Table S1 of the Supporting Information S1 as search parameters. TROPOMI data used in this study was regridded using the Python interface of the data harmonization toolset for scientific earth observation data (HARP, https://stcorp.github.io/harp/doc/html/index.html).

FRP data from the VIIRS instrument onboard the S-NPP satellite can be requested at https://firms.modaps.eosdis.nasa.gov/download/. VIIRS true color imagery with FRP information can be viewed using the Fire Information for Resource Management System (FIRMS) visualization at https://firms.modaps.eosdis.nasa.gov/map/. To view VIIRS true color imagery with FRP information or to request FRP data relevant to this study, we recommend using the wildfire starting locations and date ranges described in Table S1 of the Supporting Information S1 as search parameters.

Data from the FIREX FireLab study is available at https://csl.noaa.gov/groups/csl7/measurements/2016firex/FireLab/DataDownload/. In this study, we used open-path Fourier-transform infrared spectroscopy (FTIR) measurements of NO_2, NO, CO, and HCHO from stack burn number 37 in the FireLab. Field and laboratory emission factors from the Smoke Emissions Reference Application (SERA) are described in Prichard et al. (2020) and are available for download at https://depts.washington.edu/nwfire/sera/. Fuel type information and wildfire

emissions from version 4 of the GFED (GFED4s) are described in van der Werf et al. (2017) and can be downloaded from https://www.geo.vu.nl/~gwerf/GFED/GFED4/.

Acknowledgments
This work was supported by the National Science Foundation Graduate Research Fellowship under Grant (DGE 2040434), NOAA under Grant (NA22OAR4310538), and the NOAA GSL/CIRES Summer Research Program. This work used Copernicus data from the Sentinel-5 Precursor. The authors gratefully acknowledge those who make TROPOMI, FRP, and FIREX-AQ data available. Additionally, we thank NASA ARSET for their training on the analysis of NO_2 observations from TROPOMI, which is available in Follette-Cook and Gupta (2019).

References

Abatzoglou, J. T., & Williams, A. P. (2016). Impact of anthropogenic climate change on wildfire across western US forests. *Proceedings of the National Academy of Sciences of the United States of America*, *113*(42), 11770–11775. https://doi.org/10.1073/pnas.1607171113

Akagi, S. K., Yokelson, R. J., Wiedinmyer, C., Alvarado, M. J., Reid, J. S., Karl, T., et al. (2011). Emission factors for open and domestic biomass burning for use in atmospheric models. *Atmospheric Chemistry and Physics*, *11*(9), 4039–4072. https://doi.org/10.5194/acp-11-4039-2011

Alvarado, L. M., Richter, A., Vrekoussis, M., Hilboll, A., Kalisz Hedegaard, A. B., Schneising, O., & Burrows, J. P. (2020). Unexpected long-range transport of glyoxal and formaldehyde observed from the Copernicus Sentinel-5 Precursor satellite during the 2018 Canadian wildfires. *Atmospheric Chemistry and Physics*, *20*(4), 2057–2072. https://doi.org/10.5194/acp-20-2057-2020

Anderson, L., Dix, B., & de Gouw, J. (2023). Wildfire information and trace gas enhancement ratios (v1.0) [Dataset]. Zenodo. https://doi.org/10.5281/zenodo.8388548

Andreae, M. O. (2019). Emission of trace gases and aerosols from biomass burning—An updated assessment. *Atmospheric Chemistry and Physics*, *19*(13), 8523–8546. https://doi.org/10.5194/acp-19-8523-2019

Balch, J. K., Bradley, B. A., Abatzoglou, J. T., Chelsea Nagy, R., Fusco, E. J., & Mahood, A. L. (2017). Human-started wildfires expand the fire niche across the United States. *Proceedings of the National Academy of Sciences of the United States of America*, *114*(11), 2946–2951. https://doi.org/10.1073/pnas.1617394114

Benjamin, S. G., Weygandt, S. S., Brown, J. M., Hu, M., Alexander, C. R., Smirnova, T. G., et al. (2016). A North American hourly assimilation and model forecast cycle: The rapid refresh. *Monthly Weather Review*, *144*(4), 1669–1694. https://doi.org/10.1175/MWR-D-15-0242.1

Bertschi, I., Yokelson, R. J., Ward, D. E., Babbitt, R. E., Susott, R. A., Goode, J. G., & Hao, W. M. (2003). Trace gas and particle emissions from fires in large diameter and belowground biomass fuels. *Journal of Geophysical Research*, *108*(13), 8472. https://doi.org/10.1029/2002jd002100

Burling, I. R., Yokelson, R. J., Akagi, S. K., Urbanski, S. P., Wold, C. E., Griffith, D. W., et al. (2011). Airborne and ground-based measurements of the trace gases and particles emitted by prescribed fires in the United States. *Atmospheric Chemistry and Physics*, *11*(23), 12197–12216. https://doi.org/10.5194/acp-11-12197-2011

Burling, I. R., Yokelson, R. J., Griffith, D. W., Johnson, T. J., Veres, P., Roberts, J. M., et al. (2010). Laboratory measurements of trace gas emissions from biomass burning of fuel types from the southeastern and southwestern United States. *Atmospheric Chemistry and Physics*, *10*(22), 11115–11130. https://doi.org/10.5194/acp-10-11115-2010

Calahorrano, J. F. J., Payne, V. H., Kulawik, S., Ford, B., Flocke, F., Campos, T., & Fischer, E. V. (2021). Evolution of acyl peroxynitrates (PANs) in wildfire smoke plumes detected by the cross-track infrared sounder (CrIS) over the western U.S. during summer 2018. *Geophysical Research Letters*, *48*(23), e2021GL093405. https://doi.org/10.1029/2021GL093405

Coggon, M. M., Veres, P. R., Yuan, B., Koss, A., Warneke, C., Gilman, J. B., et al. (2016). Emissions of nitrogen-containing organic compounds from the burning of herbaceous and arboraceous biomass: Fuel composition dependence and the variability of commonly used nitrile tracers. *Geophysical Research Letters*, *43*(18), 9903–9912. https://doi.org/10.1002/2016GL070562

Copernicus Sentinel-5P. (2018a). *TROPOMI level 2 carbon monoxide total column products. Version 01*. European Space Agency. https://doi.org/10.5270/S5P-1hkp7rp

Copernicus Sentinel-5P. (2018b). TROPOMI level 2 nitrogen dioxide total column products. Version 01. https://doi.org/10.5270/S5P-s4ljg54

Copernicus Sentinel-5P. (2020). *TROPOMI level 2 formaldehyde total column products. Version 02*. European Space Agency. https://doi.org/10.5270/S5P-vg1i7t0

Copernicus Sentinel-5P. (2021a). *TROPOMI level 2 Carbon Monoxide total column products. Version 02*. European Space Agency. https://doi.org/10.5270/S5P-bj3nry0

Copernicus Sentinel-5P. (2021b). TROPOMI level 2 nitrogen dioxide total column products. Version 02. https://doi.org/10.5270/S5P-9bnp8q8

Dennison, P. E., Brewer, S. C., Arnold, J. D., & Moritz, M. A. (2014). Large wildfire trends in the western United States, 1984-2011. *Geophysical Research Letters*, *41*(8), 2928–2933. https://doi.org/10.1002/2014GL059576

De Smedt, I., Pinardi, G., Vigouroux, C., Compernolle, S., Bais, A., Benavent, N., et al. (2021). Comparative assessment of TROPOMI and OMI formaldehyde observations and validation against MAX-DOAS network column measurements. *Atmospheric Chemistry and Physics*, *21*(16), 12561–12593. https://doi.org/10.5194/acp-21-12561-2021

Deutschmann, T., Beirle, S., Frieß, U., Grzegorski, M., Kern, C., Kritten, L., et al. (2011). The Monte Carlo atmospheric radiative transfer model McArtim: Introduction and validation of Jacobians and 3D features. *Journal of Quantitative Spectroscopy and Radiative Transfer*, *112*(6), 1119–1137. https://doi.org/10.1016/j.jqsrt.2010.12.009

Follette-Cook, M., & Gupta, P. (2019). High resolution NO_2 monitoring from space with TROPOMI. Retrieved from https://appliedsciences.nasa.gov/join-mission/training/english/arset-high-resolution-no2-monitoring-space-tropomi

Fredrickson, C. D., Theys, N., & Thornton, J. A. (2023). Satellite evidence of HONO/NO_2 increase with fire radiative power. *Geophysical Research Letters*, *50*(17), 1–9. https://doi.org/10.1029/2023GL103836

Grant, E., & Runkle, J. D. (2022). Long-term health effects of wildfire exposure: A scoping review. *The Journal of Climate Change and Health*, *6*, 100110. https://doi.org/10.1016/j.joclim.2021.100110

Grell, G. A., Peckham, S. E., Schmitz, R., McKeen, S. A., Frost, G., Skamarock, W. C., & Eder, B. (2005). Fully coupled "online" chemistry within the WRF model. *Atmospheric Environment*, *39*(37), 6957–6975. https://doi.org/10.1016/j.atmosenv.2005.04.027

Griffin, D., McLinden, C., Dammers, E., Adams, C., Stockwell, C., Warneke, C., et al. (2021). Biomass burning nitrogen dioxide emissions derived from space with TROPOMI: Methodology and validation. *Atmospheric Measurement Techniques Discussions*, (2), 1–44. https://doi.org/10.5194/amt-2021-223

Jaffe, D. A., & Wigder, N. L. (2012). Ozone production from wildfires: A critical review. *Atmospheric Environment*, *51*, 1–10. https://doi.org/10.1016/j.atmosenv.2011.11.063

Jin, X., Zhu, Q., & Cohen, R. C. (2021). Direct estimates of biomass burning NOx emissions and lifetimes using daily observations from TROPOMI. *Atmospheric Chemistry and Physics*, *21*(20), 15569–15587. https://doi.org/10.5194/acp-21-15569-2021

Juncosa Calahorrano, J. F., Lindaas, J., O'Dell, K., Palm, B. B., Peng, Q., Flocke, F., et al. (2021). Daytime oxidized reactive nitrogen partitioning in western U.S. wildfire smoke plumes. *Journal of Geophysical Research: Atmospheres*, *126*(4), 1–22. https://doi.org/10.1029/2020JD033484

Landgraf, J., Aan De Brugh, J., Scheepmaker, R., Borsdorff, T., Hu, H., Houweling, S., et al. (2016). Carbon monoxide total column retrievals from TROPOMI shortwave infrared measurements. *Atmospheric Measurement Techniques*, *9*(10), 4955–4975. https://doi.org/10.5194/amt-9-4955-2016

Liao, J., Wolfe, G., Hannun, R., St. Clair, J., Hanisco, T., Gilman, J., et al. (2021). Formaldehyde evolution in U.S. wildfire plumes during FIREX-AQ. *Atmospheric Chemistry and Physics Discussions*, 1–38. https://doi.org/10.5194/acp-2021-389

Lindaas, J., Pollack, I. B., Garofalo, L. A., Pothier, M. A., Farmer, D. K., Kreidenweis, S. M., et al. (2021). Emissions of reactive nitrogen from western U.S. wildfires during summer 2018. *Journal of Geophysical Research: Atmospheres*, *126*(2), 1–21. https://doi.org/10.1029/2020JD032657

Liu, X., Huey, L. G., Yokelson, R. J., Selimovic, V., Simpson, I. J., Müller, M., et al. (2017). Airborne measurements of western U.S. wildfire emissions: Comparison with prescribed burning and air quality implications. *Journal of Geophysical Research: Atmospheres*, *122*(11), 6108–6129. https://doi.org/10.1002/2016JD026315

Prichard, S. J., O'Neill, S. M., Eagle, P., Andreu, A. G., Drye, B., Dubowy, J., et al. (2020). Wildland fire emission factors in North America: Synthesis of existing data, measurement needs and management applications. *International Journal of Wildland Fire*, *29*(2), 132–147. https://doi.org/10.1071/WF19066

Reid, C. E., Brauer, M., Johnston, F. H., Jerrett, M., Balmes, J. R., & Elliott, C. T. (2016). Critical review of health impacts of wildfire smoke exposure. *Environmental Health Perspectives*, *124*(9), 1334–1343. https://doi.org/10.1289/ehp.1409277

Roberts, J. M., Stockwell, C. E., Yokelson, R. J., De Gouw, J., Liu, Y., Selimovic, V., et al. (2020). The nitrogen budget of laboratory-simulated western US wildfires during the FIREX 2016 Fire Lab study. *Atmospheric Chemistry and Physics*, *20*(14), 8807–8826. https://doi.org/10.5194/acp-20-8807-2020

Rowe, J. P., Zarzana, K. J., Kille, N., Borsdorff, T., Goudar, M., Lee, C. F., et al. (2022). Carbon monoxide in optically thick wildfire smoke: Evaluating TROPOMI using CU airborne SOF column observations. *ACS Earth and Space Chemistry*, *6*(7), 1799–1812. https://doi.org/10.1021/acsearthspacechem.2c00048

Schnell, J., & Ahmadov, R. (2023). RAP-Chem model output for the Beckwourth Complex fire (v1.0) [Dataset]. Zenodo. https://doi.org/10.5281/zenodo.8231113

Sekimoto, K., Koss, A. R., Gilman, J. B., Selimovic, V., Coggon, M. M., Zarzana, K. J., et al. (2018). High-and low-temperature pyrolysis profiles describe volatile organic compound emissions from western US wildfire fuels. *Atmospheric Chemistry and Physics*, *18*(13), 9263–9281. https://doi.org/10.5194/acp-18-9263-2018

Selimovic, V., Yokelson, R. J., Warneke, C., Roberts, J. M., de Gouw, J. A., & Griffith, D. W. T. (2018). Aerosol optical properties and trace gas emissions from laboratory-simulated western US wildfires. *Atmospheric Chemistry and Physics*, *18*(4), 2929–2948. https://doi.org/10.5194/acp-18-2929-2018

Sokolik, I. N., Soja, A. J., DeMott, P. J., & Winker, D. (2019). Progress and challenges in quantifying wildfire smoke emissions, their properties, transport, and atmospheric impacts. *Journal of Geophysical Research: Atmospheres*, *124*(23), 13005–13025. https://doi.org/10.1029/2018JD029878

Theys, N., Volkamer, R., Müller, J. F., Zarzana, K. J., Kille, N., Clarisse, L., et al. (2020). Global nitrous acid emissions and levels of regional oxidants enhanced by wildfires. *Nature Geoscience*, *13*(10), 681–686. https://doi.org/10.1038/s41561-020-0637-7

Torres, O. (2021). TROPOMI/Sentinel-5P near UV aerosol optical depth and single scattering albedo L2 1-orbit snapshot 7.5 km x 3 km. https://doi.org/10.5067/MEASURES/AER/DATA204

Torres, O., Jethva, H., Ahn, C., Jaross, G., & Loyola, D. G. (2020). TROPOMI aerosol products: Evaluation and observations of synoptic-scale carbonaceous aerosol plumes during 2018-2020. *Atmospheric Measurement Techniques*, *13*(12), 6789–6806. https://doi.org/10.5194/amt-13-6789-2020

van der Velde, I. R., van der Werf, G. R., Houweling, S., Eskes, H. J., Pepijn Veefkind, J., Borsdorff, T., & Aben, I. (2021). Biomass burning combustion efficiency observed from space using measurements of CO and NO_2 by the TROPOspheric Monitoring Instrument (TROPOMI). *Atmospheric Chemistry and Physics*, *21*(2), 597–616. https://doi.org/10.5194/acp-21-597-2021

van der Werf, G. R., Randerson, J. T., Giglio, L., van Leeuwen, T. T., Chen, Y., Rogers, B. M., et al. (2017). Global fire emissions estimates during 1997-2016. *Earth System Science Data*, *9*(2), 697–720. https://doi.org/10.5194/essd-9-697-2017

van Geffen, J. H. G. M., Eskes, H., Boersma, K. F., & Veefkind, J. P. (2022). *TROPOMI ATBD of the total and tropospheric NO_2 data products*. S5P-KNMI-L2-0005-RP.

Veefkind, J. P., Aben, I., McMullan, K., Förster, H., de Vries, J., Otter, G., et al. (2012). TROPOMI on the ESA Sentinel-5 Precursor: A GMES mission for global observations of the atmospheric composition for climate, air quality and ozone layer applications. *Remote Sensing of Environment*, *120*, 70–83. https://doi.org/10.1016/j.rse.2011.09.027

Westerling, A. L., Hidalgo, H. G., Cayan, D. R., & Swetnam, T. W. (2006). Warming and earlier spring increase western U.S. forest wildfire activity. *Science*, *313*(5789), 940–943. https://doi.org/10.1126/science.1128834

Wooster, M. J., Freeborn, P. H., Archibald, S., Oppenheimer, C., Roberts, G. J., Smith, T. E., et al. (2011). Field determination of biomass burning emission ratios and factors via open-path FTIR spectroscopy and fire radiative power assessment: Headfire, backfire and residual smouldering combustion in African savannahs. *Atmospheric Chemistry and Physics*, *11*(22), 11591–11615. https://doi.org/10.5194/acp-11-11591-2011

Xu, L., Crounse, J. D., Vasquez, K. T., Allen, H., Wennberg, P. O., Bourgeois, I., et al. (2021). Ozone chemistry in western U.S. wildfire plumes. *Science Advances*, *7*(50). https://doi.org/10.1126/sciadv.abl3648

Yates, E. L., Iraci, L. T., Singh, H. B., Tanaka, T., Roby, M. C., Hamill, P., et al. (2016). Airborne measurements and emission estimates of greenhouse gases and other trace constituents from the 2013 California Yosemite Rim wildfire. *Atmospheric Environment*, *127*, 293–302. https://doi.org/10.1016/j.atmosenv.2015.12.038

Yokelson, R. J., Griffith, D. W., & Ward, D. E. (1996). Open-path Fourier transform infrared studies of large-scale laboratory biomass fires. *Journal of Geophysical Research*, *101*(15), 21067–21080. https://doi.org/10.1029/96jd01800

Zoogman, P., Liu, X., Suleiman, R. M., Pennington, W. F., Flittner, D. E., Al-Saadi, J. A., et al. (2017). Tropospheric emissions: Monitoring of pollution (TEMPO). *Journal of Quantitative Spectroscopy and Radiative Transfer*, *186*, 17–39. https://doi.org/10.1016/j.jqsrt.2016.05.008